 doi:10.20944/preprints202105.0363.v1

Experimental Dental Composites Containing a Novel Methacrylate-Functionalized Calcium Phosphate Component: Evaluation of Bioactivity and Physical Properties

Sunny Skaria, Kenneth J. Berk

Sunny Skaria, PhD
Research Scientist
Pulpdent Corporation
80 Oakland Street
Watertown, MA 02472
USA

Kenneth J. Berk
Director R&D
Pulpdent Corporation
80 Oakland Street
Watertown, MA 02472
USA

Address for Correspondence:

Sunny Skaria, PhD
Pulpdent Corporation
80 Oakland Street
Watertown, MA 02472
USA
Email: sunny@pulpdent.com

 doi:10.20944/preprints202105.0363.v1

Abstract:

The aim of this study was to synthesize and characterize a novel Methacrylate-functionalized Calcium Phosphate (MCP) used as a bioactive compound for innovative dental composites. The characterization was accomplished by Attenuated Total Reflectance Fourier-Transform Infrared Spectroscopy (ATR-FTIR), X-Ray Diffraction Analysis (XRDA), Scanning Electron Microscopy (SEM), and EnergyDispersive Spectroscopy (EDS). The incorporation of MCP as a bioactive filler in esthetic dental composite formulations and the ability of MCP containing dental composites to promote precipitation of hydroxyapatite (HAp) on the surfaces of those dental composites was explored. The translucency parameter, depth of cure, degree of conversion, ion release profile, and other physical properties of composites were studied with respect to the amount of MCP added to the composites. Composites containing 3 Wt.%, 6 Wt.%, and 20 Wt.% MCP were evaluated at 7, 14, and 21 days. The progress of surface precipitation of hydroxyapatite on MCP-containing dental composites was studied by systematically increasing the MCP content in the composite and the time of specimen storage in Dulbecco's phosphate-buffered solution with calcium and magnesium. It was found that there was a direct correlation between the percentage of MCP in a composite formulation, the amount of time the specimen was stored in PBS, and the deposition of hydroxyapatite on the composite's surface.

Keywords:

Dental composite

Methacrylated calcium phosphate

Biomineralization

 doi:10.20944/preprints202105.0363.v1

Introduction:

Natural bone and teeth are unique composites of biological origin. They consist of a mineral inorganic phase of calcium-phosphates and an organic phase of collagen. Dentin is a mineralized structure that forms the major component of dental hard tissue. It is covered by a highly mineralized and protective layer of enamel in the crown and cementum in the root [1, 2].

Demineralization and remineralization processes co-exist in teeth during the entire life of an individual [3]. Dental caries is a dynamic disease process caused by the imbalance of demineralization and remineralization. It occurs in pathological conditions when demineralization outweighs remineralization. The dental caries process begins with demineralization of apatite by acids produced by oral biofilm bacteria (plaque), followed by the degradation of the extracellular organic matrix of dentin. As caries progresses, degradation of collagen fibrils occurs and leads to a decrease in the mechanical properties of the dentin [4, 5]. In general, the caries process is initially a reversible, chronic condition that progresses slowly; it can be arrested by disturbing the plaque biofilm. [6].

Remineralization of carious dentin can occur either by a spontaneous incorporation of beneficial ions, such as calcium, phosphate and fluoride, from the oral fluid into remnant crystallites in the demineralized tissue, or by treatments that incorporate the same beneficial ions from external sources. The repair of dental caries with dental restoratives (fillings) that release calcium, phosphates and fluoride ions is gaining interest. These bioactive restoratives can help prevent caries by inducing the remineralization of hypo-mineralized caries lesions and by interfering with the metabolic activity of the biofilm [7, 8, 9].

Dental resins containing calcium phosphate fillers such as hydroxyapatite (HAp), amorphous calcium phosphates, nano-calcium phosphates, and mono-, di- and tetra-calcium phosphates have

 doi:10.20944/preprints202105.0363.v1

been investigated in past years as calcium and phosphate releasing composites with remineralizing capabilities [10, 11, 12]. Dental composites containing amorphous calcium phosphate release super-saturated levels of calcium and phosphate ions and have been shown to remineralize tooth lesions *in vitro* [13, 14].

Recently, a combination of reactive calcium dihydrogen phosphate and tri-calcium phosphate has been used. The less soluble tri-calcium phosphate enhances control over the composite's water absorption and the dissolution of the more soluble calcium dihydrogen phosphate [15]. A light-curable composite containing systematically varying amounts of calcium dihydrogen phosphate, tri-calcium phosphate, and chlorhexidine was investigated for its bioactivity and antibacterial properties [16]. However, the high amounts of calcium phosphate in formulations reduces the tooth-mimicking esthetics required for successful dental composites, and the low compatibility of the resin phase with the CaP fillers reduces the mechanical properties [17].

Several strategies to increase the interaction of these bioactive fillers with resin phases have been tested. These include (i) silane coupled HAp [18]; (ii) nano-sized amorphous calcium phosphate (NACP) [19, 20]; and or (iii) the functionalization of calcium phosphate particles with dimethacrylate monomers [21, 22]. Modest improvement in fracture strength was observed in resin composites containing functionalized fillers in comparison to those containing non-functionalized brushite [23].

A great surge of interest in bioactive dental materials was observed in 2013 after the introduction of the first esthetic, bioactive, dental restorative material, Activa Bioactive-Restorative (AB) (Pulpdent Corporation, Watertown, MA, USA). AB is composed of a reactive, ionic resin (bis-2-(methacryloyloxy)ethyl phosphate) (Bis-2), polycarboxylic acid, and reactive glass. It releases and recharges beneficial calcium, phosphate, and fluoride ions [24], which

Preprints (www.preprints.org) | NOT PEER-REVIEWED | Posted: 16 May 2021 doi:10.20944/preprints202105.0363.v1

facilitate remineralization and reduce demineralization of dentinal tissues [25]. In addition to the incorporation of elements for bioactivity, AB materials also contain a rubberized polyurethane-methacrylate-resin that increases fracture toughness and mimics the toughness of dentin [26]. AB facilitates surface precipitation of calcium phosphate, has high tissue compatibility, and induces new osteogenic bone growth [27, 28, 29]. In these materials, the calcium and phosphate ions are released from the ionomer glass by the reaction of the ionic resin with the ionomer glass.

The original AB materials require a two-part system to derive the benefit of the glass ionomer reaction. To achieve bioactive properties in a one-part material, the authors synthesized Methacrylate-functionalized Calcium Phosphate (MCP), a calcium phosphate with pendent methacrylate groups. Composites incorporating MCP can be formulated as one-part, light-cure only materials. Although dental composites containing varying amounts of bioactive fillers, such as Bioglass or calcium phosphate, have been studied, the application of a methacrylate-functionalized calcium phosphate and its commercial development as esthetic bioactive composites is hitherto unknown. This study investigates the bioactivity of methacrylate-functionalized calcium phosphate containing composites in a concentration dependent manner and the effect of MCP on the optical and physical properties of the composites.

2. Materials and Methods:

2.1 Materials

2.1.1 Methacrylate-functionalized Calcium Phosphate (MCP)

The methacrylate-functionalized calcium phosphate (MCP) was synthesized by the conventional solution-precipitation chemistry method, reacting calcium salts with a mixture of phosphoric acid and the phosphate-functional monomer, Bis-2. MCP was precipitated from the solution phase by bringing the pH to 10 with the addition of an ammonia solution. The resultant

Preprints (www.preprints.org) | NOT PEER-REVIEWED | Posted: 16 May 2021 doi:10.20944/preprints202105.0363.v1

MCP was filtered, washed with distilled water, and dried at 45ºC. The powder was then ball milled for 1h and sifted. The powder was analyzed by FTIR-ATR, XRD, SEM and EDS [30].

2.1.2 Synthesis of Polymer Composites

The bioactive ionic resin formulation used in the tested composites contains aliphatic urethane dimethacrylate and other multi-methacrylate monomers. The resin also contains a patented rubberized urethane methacrylate resin [31]. to provide additional toughness and durability to the composite. The experimental composites are 70% filled with a mixture of radiopaque, silanated barium and strontium alumino-silicate glasses with an average particle size of 0.7µm to 4µm and submicron silica fillers. They contain varying amounts of methacrylate-functionalized calcium phosphate (MCP) as the bioactive filler and 0.4 Wt.% other additives (CQ-amine initiator system and colorants). The mixing of the resins and the powders was carried out in a Ross mixer (Charles Ross & Sons, NY, USA).

To determine the optimum levels of MCP required for bioactivity and esthetics, and to understand the relationship between MCP concentrations in the composite and its bioactivity and mineralization properties, formulations with 3%, 6% and 20% MCP and a control composite with no MCP were investigated for their ion release and physico-chemical properties.. All of the specimens were polymerized by light curing with a light source having an output of 600 mW/cm^2 (LE Demetron, Kerr, Orange, CA, USA), and the intensity was frequently measured with a hand-held radiometer (Demetron, Kerr, Orange, CA, USA). All formulations were shaded to a Vita A2 shade to enable an unvarying comparison of the optical and physical properties. The composite formulations are presented in Table **1**.

Preprints (www.preprints.org) | NOT PEER-REVIEWED | Posted: 16 May 2021 doi:10.20944/preprints202105.0363.v1

Table 1: Composite Formulations

Sample	TFC %	Resin Matrix %	MCP %	CQ %
Control Comp, 0% MCP(**CS-0**)	69.5	30	0	0.08
Comp + 3Wt.% MCP (**CS-3**)	69.5	30	3	0.08
Comp + 6Wt.% MCP (**CS-6**)	70.4	29	6	0.08
Comp + 20Wt.% MCP (**CS-20**)	74.4	25.5	20	0.08

TFC %: Total Filler Content % includes Barium/Strontium alumino silicate, Silica, and MCP.

2.2 Physico-Chemical Characterization

2.2.1. FTIR characterization

Attenuated Total Reflection Fourier Transform Spectroscopy (ATR-FTIR) was employed to characterize the methacrylate-functionalized calcium phosphate (MCP) and the precipitated layer formed on the composite after immersion in PBS. The spectra of the specimens were obtained using a Nicolet IR200 spectrophotometer (Thermo-Fisher, Waltham, MA, USA) with an ATR accessory and were recorded in absorption mode using 4 cm^{-1} resolution in the range of 500-4000 cm^{-1}. The FTIR of the surface precipitated layer was measured by scraping off that layer from the specimens after being stored in phosphate buffered saline (PBS) for 21 days at 37°C.

2.2.2. Translucency Parameter

The translucency parameter (TP) was calculated from the color coordinate values of the composite material [32]. The color of the composite materials was measured using a reflection spectrophotometer. Specimens 9 mm in diameter and 2 mm in thickness (N=3) were fabricated in a silicon mold. Each specimen was light cured for 20 seconds on each side. Each specimen was polished to a thickness of 2 mm on a 600 Grit SiC paper measured by a digital micrometer

Preprints (www.preprints.org) | NOT PEER-REVIEWED | Posted: 16 May 2021 doi:10.20944/preprints202105.0363.v1

(Mitutoyo, Japan). The color of each specimen was measured according to the CIELAB color scale (color notation system developed by Commission Internationale de l'Eclairage), and related to the standard illuminant D65 against a white background and a black background using a reflection spectrophotometer (Color i7 spectrophotometer, XRite Corp, Grand Rapids, MI, USA). After determining the color of the specimen, the translucency parameter (TP) was calculated by the difference between the color of the specimen over the white background and the color of the specimen over the black background using the following equation:

$$\mathbf{TP= [(L_w-L_b)^2 + (a_w-a_b)^2 + (b_w-b_b)^2]^{1/2}}$$

Where **L** is the coordinate for the lightness; **a** (green/red) and **b** (blue/yellow) are chromatic coordinates; the subscript *b* refers to color parameters over the black background; and subscript *w* refers to color parameters over the white background.

2.2.3. Degree of Conversion (DC)

The degree of conversion of the composites with respect to the amount of the MCP filler in the formulation was evaluated.

Prior to curing, the specimens were fabricated in black silicon molds 1 mm in height and 4 mm in internal diameter placed directly on the ATR cell of the ATR-FTIR spectrophotometer (Nicolet IR 200, Thermo-Fisher, Waltham, MA, USA). A transparent Mylar film was placed over the material, and the spectrum of the specimens were recorded before light activation.

After light curing the specimen from the top surface for 20 seconds, the spectrum of the bottom layer of each polymerized specimen was scanned. More scans of the bottom layer were recorded after irradiating the specimen at the top surface for 40, 60, and 120 seconds.

Preprints (www.preprints.org) | NOT PEER-REVIEWED | Posted: 16 May 2021 doi:10.20944/preprints202105.0363.v1

The degree of conversion of the specimens was determined by the ratio of the area of the methacrylate group (C=C) at 1638 cm^{-1} of the polymerized specimen to that of non-polymerized specimen. The DC was calculated according to the following equation [33].

$$\mathbf{DC\ (\%) = [(A_1/A_0 - A_{1'}/A_{0'}) / A_1/A_0)]\times 100,}$$

Where A_1/A_0 and $A_{1'}/A_{0'}$ are the peak area ratio of methacrylate and amide, before and after polymerization**.** The amide group of the UDMA at 1537 cm^{-1} was used as the internal standard.

2.2.4. Depth of Cure

The depth of cure of each test material was measured by ISO 4049 [34]. Specimens (N=3) of each material were made in a steel mold 4 mm in internal diameter and 6 mm in height. A transparent Mylar film was placed over it. The specimens were light cured from the top surface for 20 seconds. After curing, the specimens were immediately removed from the mold and the uncured material at the bottom surface of each specimen was scraped away using a plastic spatula. The height of the remaining specimen was measured using a digital micrometer (Mitutoyo, Japan). The ISO 4049 mean depth of cure of each material was calculated by averaging the height of the polymerized specimen of each material and dividing the average height of the specimen by two.

2.2.5: Flexural Strength (FS) and Deflection at Break

Six specimen bars with dimensions of 2×2×25 mm were fabricated for each material by injecting the material into a polypropylene mold. The mold was placed between two glass sides covered with Mylar film. The specimen bars were cured for 1 minute on each side using a light source of 600 mW/cm^2. After curing, the specimen bars were taken out of the mold, excess flash was removed, and the specimens were wet polished with 600 Grit paper. The specimens were then stored in PBS for one day at 37°C. The specimen dimensions were measured by a digital micrometer of 0.01 mm sensitivity (Mitutoyo, Japan). Immediately after removing the specimens

Preprints (www.preprints.org) | NOT PEER-REVIEWED | Posted: 16 May 2021 doi:10.20944/preprints202105.0363.v1

from the PBS, the three-point flexural strengths of the specimen bars were tested on a Universal testing machine (Instron T1140, Norwood, MA, USA) with a cross head speed of 1mm/min. The distance between the support beams of the three point jig was 20 mm. Flexural Strength (FS) in MPa was calculated using the following equation:

FS = PMax.3L/2bh^2, where Pmax is the load at break, b is the specimen width, h is the specimen thickness, and L=20.

The deflection of break data for each specimen was generated from the three-point flexural strength measurements and was measured by correlating the crosshead motion to beam deflection.

2.2.6. Ion Release studies

Disk shaped specimens (N=5) approximately 9 mm in diameter and 2.5 mm in thickness were fabricated by injecting the composite material into a silicon mold and light curing for 20 seconds on each side. The dimensions of each specimen were then accurately measured using the digital micrometer, and the weight of each specimen was recorded. Each specimen was stored in 10 mL of distilled water (pH 7) in an incubator (Boekel Industries, Feasterville, PA, US) at 37°C. After 24 hours, each specimen was transferred to a new bottle with 10 mL of fresh distilled water.

The calcium ions present in the solution of the original bottle were measured by UV-Vis colorimetric analysis (Genesis 10S UV-Vis, Thermo Scientific, Waltham, MA, USA), after an aliquot of the solution was treated with cresolphthalein-complexone reagent (Aldrich, Milwaukee, USA) [35]. To calibrate, UV-Vis spectrophotometer standard calcium ion solutions in the concentration ranges of 0.2, 0.4, 1.0, 2.0, 5.0 and 10 ppm were used. The procedure was repeated and the calcium ion release from the specimens was calculated on days 2, 5, 7, 14, 21 and 28.

The release of phosphate ions was measured by colorimetric analysis using Smart 2 Colorimeter (LaMotte, MD, USA) after complexing with Vanadate Molybdate reagent (Aldrich,

Preprints (www.preprints.org) | NOT PEER-REVIEWED | Posted: 16 May 2021 doi:10.20944/preprints202105.0363.v1

Milwaukee, USA). The specimens (N=5) were stored in 10 mL of distilled water, and the soluble phosphate ions in the solution on day was determined. The procedure was repeated, and the ion release from the specimens was calculated on days 2, 5, 7, 14, 21 and 28. Calibration curves were generated by 1, 2, 5, 10, 20 and 40 ppm standard solutions of sodium phosphate in distilled water.

2.3 Composite disc preparation and bioactivity studies

The *in-vitro* bioactivity and the bio-mineralization potentials of MCP containing composites were tested in accordance with ISO method 23317:2014 [36] by immersing the specimens in commercial Dulbecco's phosphate-buffered solution with calcium and magnesium (PBS) (D 8662, Sigma-Aldrich, St. Louis, MO, USA). Thirty cylindrical specimens 9 mm in diameter and approximately 3.6 mm in thickness were prepared in a two-step process. (1) A silicone mold 9 mm in diameter and approximately 1.8 mm thickness was placed on a Mylar sheet on a flat glass plate. The composites were injected into the mold, a nylon thread 6 cm long was placed across the composite, and a Mylar film and glass plate were placed on top. The specimens were light-cured for 20 seconds (LE Demetron II, Kerr, Orange, CA, USA). (2) The top glass plate and the mylar film were removed, and a second silicon mold of similar dimension to the first was placed over the cured resin and the nylon thread. The composite material was injected into the second mold. A Mylar film was placed over the material followed by a glass plate. The material was light-cured for another 20 seconds on each side of the disc (total thickness approximately 3.6 mm). The specimen disc was removed from the mold, its surfaces were polished using a 220-grit SiC paper, and it was washed with distilled water and dried. Using the nylon thread, the specimen discs were suspended vertically in plastic bottles containing 25 mL of PBS and stored at 37º C. On the 7th day, specimens were removed from the plastic bottles, washed thoroughly with distilled water, dried, and stored in a desiccator for SEM evaluation. The remaining specimens remained in their

Preprints (www.preprints.org) | NOT PEER-REVIEWED | Posted: 16 May 2021 doi:10.20944/preprints202105.0363.v1

plastic bottles, and the PBS was changed. This process was repeated for all specimens at 14 days and 21 days.

The specimens were analyzed using SEM (Amray 3300 FESEM, field emission scanning electron microscope and Energy Dispersive X-ray Spectroscopy (EDS) to assess the morphology and elemental composition of the surface precipitated layer formed on the specimens. Control specimens (0 days) and the specimens stored in PBS for 7, 14 and 21 days were mounted on aluminum SEM stubs using double-sided, carbon adhesive tape. The SEM stubs were sputter-coated with Au-Pd for 90-95 seconds in a Denton Vacuum Desk II (Moorestown, NJ, USA) to eliminate charging in non-conductive specimens. The specimens were analyzed at 10KV, condenser spot size -25, objective aperture 200, working distance of 25-28 mm, using a RaySpec light element detector (High Wycombe, UK) for 120-130 seconds to determine the elemental composition of the material. Images were captured at magnifications of 40x, 100x, 1,000x, 2,000x, 3,000x and 6,000x.

3. Results

3.1 FTIR: Characterization of MCP

The FTIR spectra of the organic functional monomer (Bis-2), the methacrylate-functionalized calcium phosphate powder (MCP), and the annealed MCP (annealed at 600^{o}C for 4 hours) are depicted in **Figure 1**.

FTIR Spectra of Bis 2 resin, MCP powder, and Annealed MCP powder

Preprints (www.preprints.org) | NOT PEER-REVIEWED | Posted: 16 May 2021 doi:10.20944/preprints202105.0363.v1

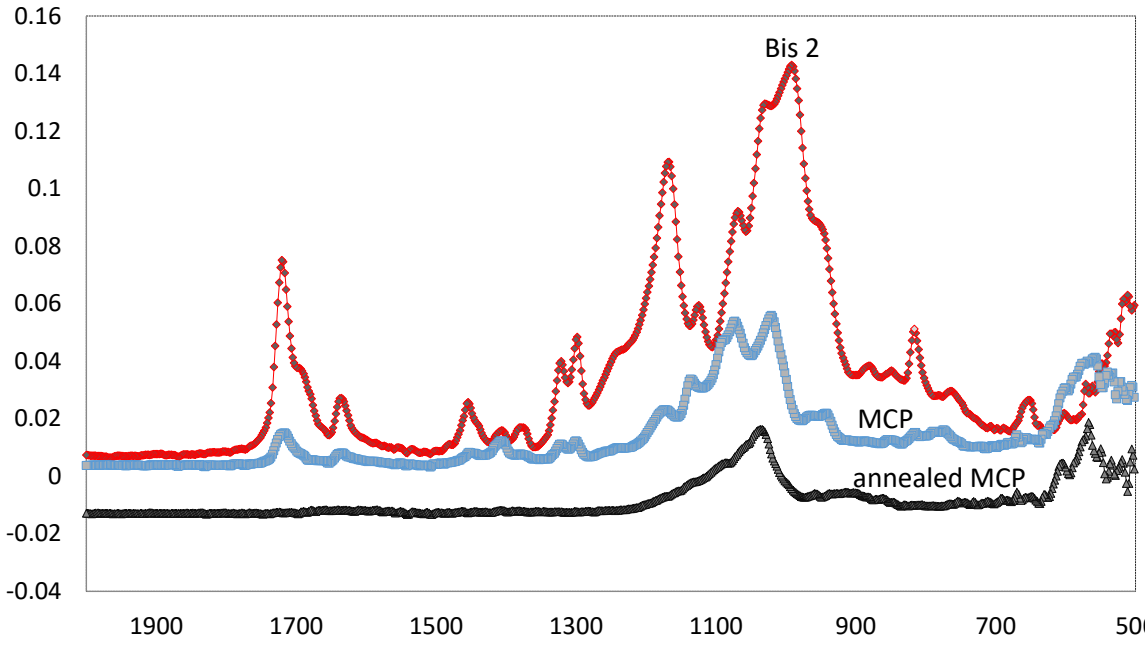

Figure 1. FTIR Spectra of Bis 2-(methacryloyloxy) ethyl phosphate (Bis 2) monomer (red line], methacrylate functionalized calcium phosphate (MCP) (blue line), and MCP annealed at 600 ºC for 4 hours (black solid line). Both Bis-2 and MCP show the characteristic absorption peak of methacrylate group (1720 cm^{-1} and 1635 cm^{-1}) and other absorption peaks originated from C-O and P-O groups (see text). The annealed MCP showed only absorption peaks characteristic of P-O groups, and it shows no peaks related to organic functional C-O groups.

The FTIR spectrum of MCP powder was very complex. The absorption peaks of MCP powder were close to, or merge with, the absorption peaks of the phosphate monomer (Bis-2), especially in the 950-1300 cm^{-1} region. The absorption peaks of MCP powder at 1720 cm^{-1}(C=O) and 1635 cm^{-1} (C=C) indicated that the methacryloyl group was already in the powder. The absorption peaks of MCP powder at 1074 cm^{-1} and 1021 cm^{-1} were attributed to the P-O vibration modes of regular tetrahedral PO_4 groups, which were also observed in the Bis-2 monomer [37].

The FTIR spectrum of the annealed MCP showed no presence of organic groups, as there were no absorption peaks observed at 1720 cm^{-1} and 1635 cm^{-1} (corresponding to the organic

Preprints (www.preprints.org) | NOT PEER-REVIEWED | Posted: 16 May 2021 doi:10.20944/preprints202105.0363.v1

monomer Bis-2). Instead, all of the characteristic peaks of HAp were increased. The FTIR of the annealed MCP showed characteristic absorption bands of HAp, evidenced by the presence of PO_4^{3-} (υ_1 963 cm^{-1}-, υ3 1039 and 1090 cm^{-1}, υ4 603 and 568 cm^{-1}). This proves the thermal degradation of both the carbonaceous group and the organic functional group upon annealing at 600℃ for 4 hours. The organic, volatile part of the MCP was calculated by weight difference to be 42% of the material.

3.2 Mechanical Properties:

The **Translucency Parameters (TP)** of the experimental composites are presented in **Table 2**. When measured with a specimen of 2 mm thickness, the 3% MCP composite presented the highest TP value of 8.6 followed by the composite with 6% MCP (8.4) and the control specimen without MCP (8.4). The commercial composite Filtek Supreme (3M) shows TP value of 7.7. The composite with 20% MCP showed the lowest TP value of 5.4. The high amount of filler in the 20% MCP composite reduces the TP value. The addition of MCP in the range of 1-6 Wt.% did not change the translucency of the composite.

The mean **Degree of Conversion (DC),** measured at the bottom surface of the specimens as a function of irradiation time, and the amount of the functional MCP filler, is shown in **Figure 2**. The DC values of the tested specimens (N=3) are calculated based on the peak area of the C=C group (1638 cm^{-1}) of the starting material, represented as 0% of conversion, versus the peak area of the polymerized specimen. The control composite (no MCP) and 3 Wt.% MCP composite showed the highest DC values, in the range of 69, and are not statistically different. The DC of the specimens decreased with the amount of added MCP in the specimen. The specimen with 20% MCP showed the lowest DC at 58%.

Preprints (www.preprints.org) | NOT PEER-REVIEWED | Posted: 16 May 2021 doi:10.20944/preprints202105.0363.v1

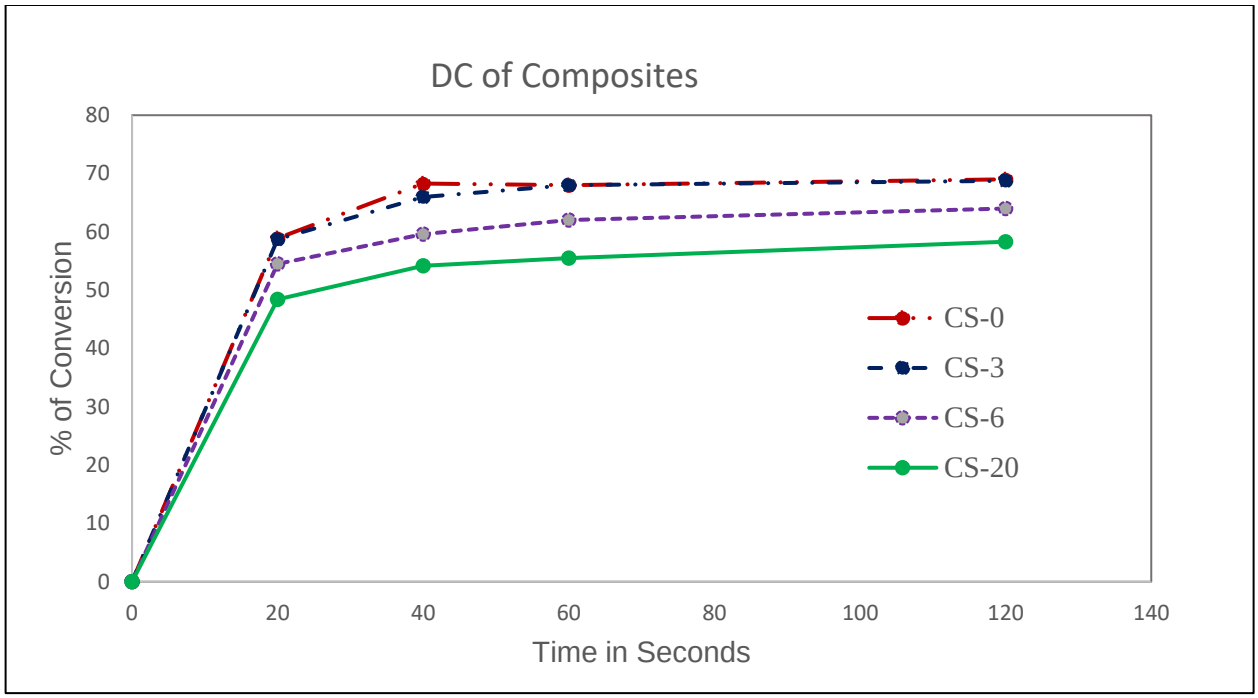

Figure 2. Degree of conversion of composites with respect to time of irradiation shows decreasing conversion rates with increasing percentages of MCP.

The mean ISO **Depth of Cure** values are also presented in **Table 2**. The ISO depth of cure of the composites ranged from 2.48 to 2.66 mm. The 3Wt.% MCP composite presented slightly higher depth of cure (2.65 mm) compared to the control composite with no MCP (2.62mm). The depth of cure for 6Wt.% MCP was 2.58 mm, and lowest depth of cure value of 2.48 mm was for the specimen with 20 Wt.% MCP.

The mean **Flexural Strength** (FS) of the composites is presented in **Table 2**. The specimen with 3Wt.% MCP presented the highest flexural strength at 106 MPa. The flexural strength values observed for the control specimen and the 6Wt.% MCP specimen were not significantly different, while the specimen with 20Wt.% had the lowest flexural strength value of 92.6 MPa.

Table 2: Physico-Chemical Properties of Composites

Preprints (www.preprints.org) | NOT PEER-REVIEWED | Posted: 16 May 2021 doi:10.20944/preprints202105.0363.v1

Sample	Depth of Cure %	Translucency Parameter (TP)	Depth of Cure (mm)	Flexural Strength MPa/ (sd)	Deflection at Break (mm)
CS-0	69	8.4	2.62	98.2 (2.8)	0.58
*CS-**3***	69	8.6	2.65	106 (3.2)	0.74
CS-6	64	8.4	2.58	99.4 (2.9)	0.75
CS-20	58	5.5	2.48	92.6 (3.8)	0.72

The **Deflection at Break** of the specimens is also presented in Table 2. The mean deflection at break for the specimens containing MCP were higher than those of the control specimen (no MCP). The highest deflection at break, 0.75mm was for specimen containing 6 Wt.% MCP; however, it was not statistically different from that of the specimens with 3 Wt.% MCP (0.74 mm) and 20 Wt.% MCP (0.72mm). The deflection at break value for the control composite with no MCP was 0.58 mm.

3.3. Calcium and Phosphate Ion Release

F**igures 3** to **5** show the cumulative release of calcium ions and phosphate ions from the composite materials as a function of time for the four weeks of the study. Specimens containing MCP showed continuous release of calcium and phosphate ions over the four-week period. The specimen containing 20 Wt.% MCP showed the highest amount of calcium and phosphate release. The cumulative calcium release from the specimen with 20 Wt.% MCP was 12 mM/L or 486 mg/cm^2, and the cumulative phosphate ion release from that specimen was 5.2 mM/L or 500 mg/cm^2. The control composite released the lowest amount of calcium and phosphate ions; those primarily originate from the inorganic glass fillers.

Preprints (www.preprints.org) | NOT PEER-REVIEWED | Posted: 16 May 2021 doi:10.20944/preprints202105.0363.v1

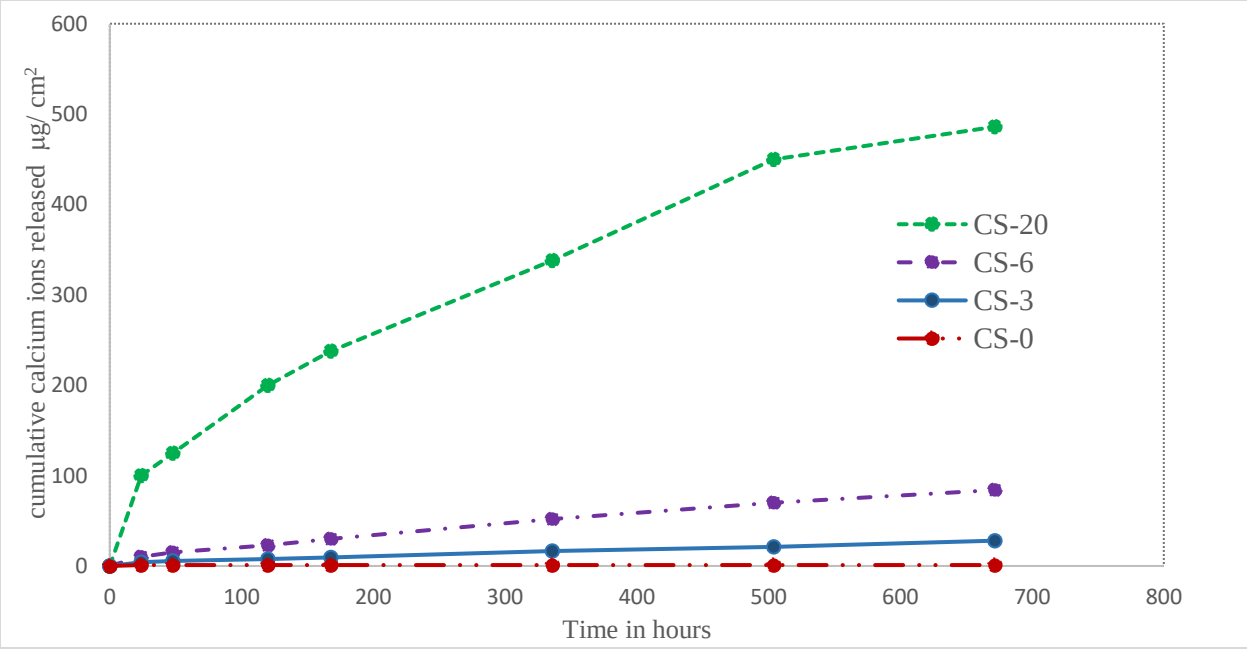

Figure 3. Cumulative release profile data calcium ions from the composite specimens shows escalating release of phosphate ions with increasing percentages of MCP

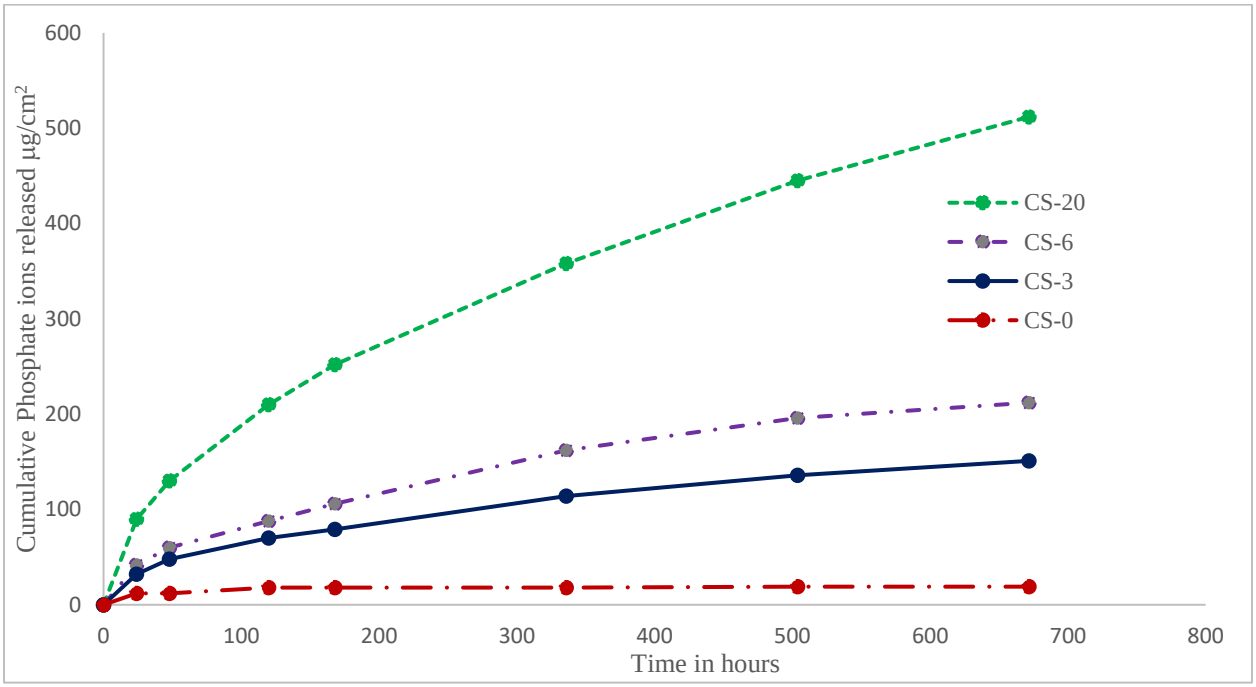

Figure 4. Cumulative release profile data of phosphate ions from the composite specimens shows escalating release of phosphate ions with increasing percentages of MCP.

Preprints (www.preprints.org) | NOT PEER-REVIEWED | Posted: 16 May 2021 doi:10.20944/preprints202105.0363.v1

Cumulative Ion Release in Four Weeks

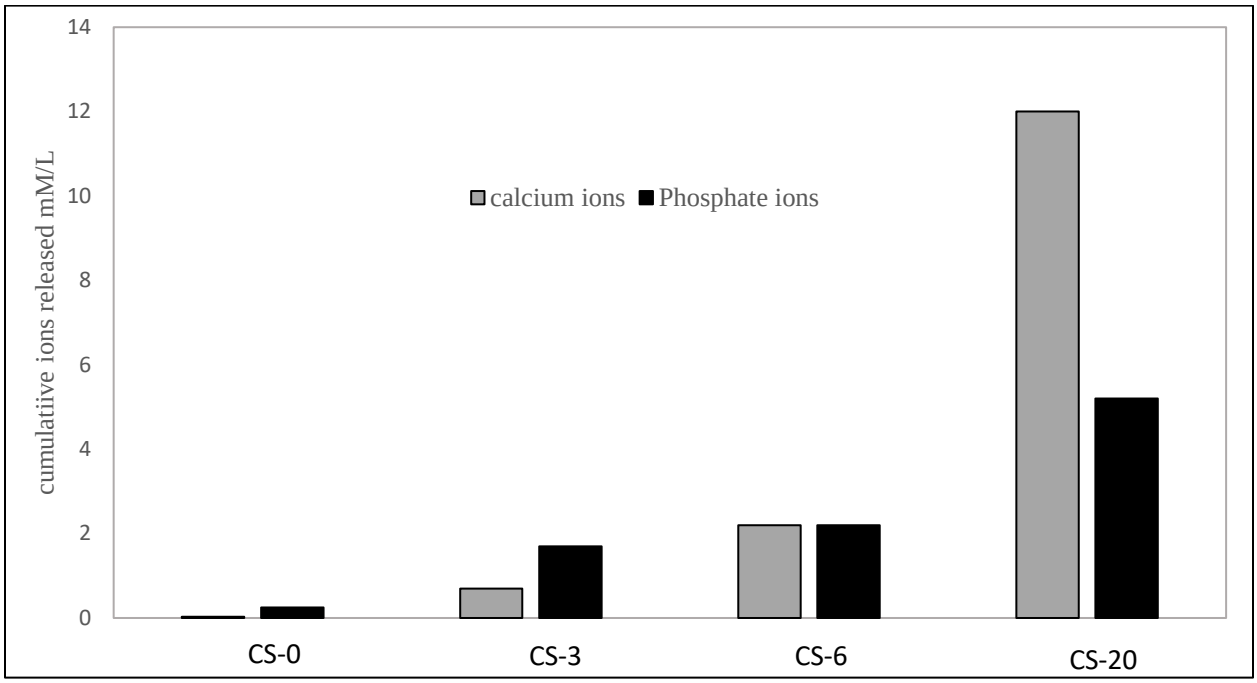

Figure 5. Cumulative ions (mM/L) released from the composite specimens over a period of four weeks shows the increasing activity of the specimens with increasing percentages of MCP

The release of calcium and phosphate ions from the various composite materials is directly correlated to the amount of MCP in the material. The relative molar mass release of calcium ions to phosphate ions decreased as the percentage of MCP filler in the composite decreased.

3.4. Bioactivity and Apatite formation:

This experiment demonstrated a direct relationship between the hydroxyapatite formation on the surface of the specimens, the percentage of MCP in the specimen, and the number of days of storage in PBS. After 21 days of storage in PBS, all the specimens showed at least partial hydroxyapatite aggregates on the specimen disc surface. As the percentage of MCP increases, there is a dramatic increase in the development of calcium phosphate crystals on the surface of the specimens. The calcium and phosphate contents of the specimens before immersion in PBS were 0.73% and 0.65% respectively.

Preprints (www.preprints.org) | NOT PEER-REVIEWED | Posted: 16 May 2021 doi:10.20944/preprints202105.0363.v1

The SEM micrographs of specimens containing 3Wt.% MCP (CS-3), before and after immersion in PBS, are presented in Figures 6A, 6C and 6E and the corresponding EDS are presented in Figures 6B, 6D and 6F. These SEMs show two distinctive and approximately equal areas of crystal growth: (1) light regions covered with aggregates of calcium phosphate and with the potential to serve as nucleation sites for further calcium phosphate deposition, and (2) dark areas where lower calcium phosphate can be observed. The EDS analysis of the light areas shows fully developed calcium phosphate crystals with a high mean Ca:P ratio and no peaks originating from the substrate polymer disk. This indicates extensive growth of apatite in those regions. The EDS analysis of the dark areas shows a five-fold increase in calcium and phosphate ion concentrations compared to the control specimen, but much lower than the light areas. The dark areas indicate immature calcium phosphate growth. **(Table 3)**

Table 3. EDS analysis of Calcium and Phosphorous atom ratios observed on the surface of Activa Presto before and after immersion in PBS for 21 days

Material	**Calcium (Ca) %**	**Phosphorous (P) %**	**Ca:P Ratio**
3Wt.% MCP (**CS-3**) before immersion in PBS (Figures 6A and 6B)	0.73	0.65	1.12
CS-3 after immersion in PBS for 21 days Light area indicates extensive CaP precipitation (see Figures 6C, 6E and 6F)	31.26	19.42	1.61
CS-3 after immersion in PBS for 21days Dark area indicates mild CaP precipitation (See Figures 6C, 6D)	2.75	2.22	1.24

Preprints (www.preprints.org) | NOT PEER-REVIEWED | Posted: 16 May 2021 doi:10.20944/preprints202105.0363.v1

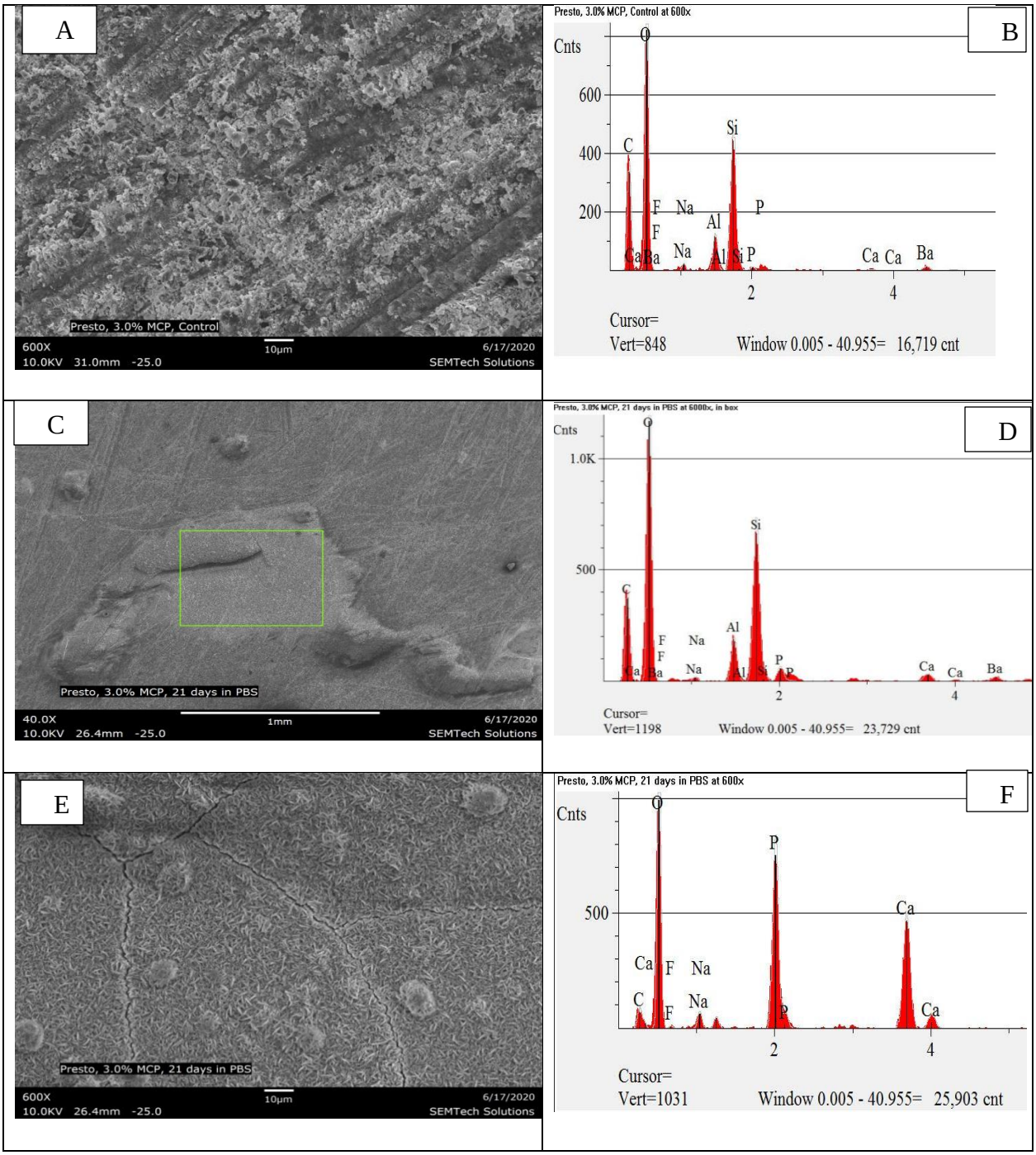

Figure 6. SEM micrograph **A** and EDS spectrum **B** of and Experimental composite with 3Wt.% MCP (**CS-3**) before immersion in PBS (600x); (**C**) SEM image of same material after 21 days of storage shows two areas of calcium phosphate precipitation, light area (box) and dark area (40x); (**D**)EDS spectrum of dark region and (**E**) SEM enlargement of the boxed area of **CS-3** 6(B) shows well-developed CaP crystals (600x) and its (**6F**) EDS spectrum.

Preprints (www.preprints.org) | NOT PEER-REVIEWED | Posted: 16 May 2021 doi:10.20944/preprints202105.0363.v1

In-order to understand the biomineralization potential of MCP as a functional filler, experimental specimens containing even higher percentages of MCP were studied. Specimens with 6 Wt.% MCP, after 7 days storage in PBS, show the entire surface of the specimen disc covered with calcium phosphate nucleation sites (**Figure 7a**). The EDS after 7 days storage in PBS shows Ca:P ratios ranging from 1.10 to 1.40, suggesting the formation of calcium deficient hydroxyapatite [38]. At 14 days, well-developed hydroxyapatite can be seen throughout the surface of the specimen (**Figure 7b)**. SEM and EDS analysis show remarkable bioactivity and HAp formation for a composite containing 20% MCP **(Figure 7c and 7d).** The calcium and phosphorous elemental concentrations obtained by EDS are presented in **Table 4.**

Table 4. EDS of 6 WT% and 20 WT% MCP materials at 6000x magnification to analyze precipitate calcium and phosphorous atom ratios on the specimen surfaces at the molecular level.

Material	**Calcium** %	**Phosphorous** %	**Ca:P Ratio**
Composite with 6% MCP (CS-6) control (not immersed in PBS) (6,000x)	2.6	2.5	1.03
CS-6 after 7 days immersion in PBS (6,000x)	29.81	21.79	1.37
CS-6 after 14 days immersion in PBS (6,000x)	31.64	20.39	1.55
CS-6 after 21 days immersion in PBS (6,000x)	30.52	19.63	1.56
Composite with 20% MCP (CS-20) control (not immersed in PBS) (6,000x)	8.4	6.9	1.22
CS-20 after 7 days immersion in PBS (6,000x)	27.07	20.25	1.34
CS-20 after 14 days immersion in PBS (6,000x)	30.12	19.62	1.54
CS-20 after 21 days immersion in PBS (6,000x)	32.49	20.31	1.60

Preprints (www.preprints.org) | NOT PEER-REVIEWED | Posted: 16 May 2021 doi:10.20944/preprints202105.0363.v1

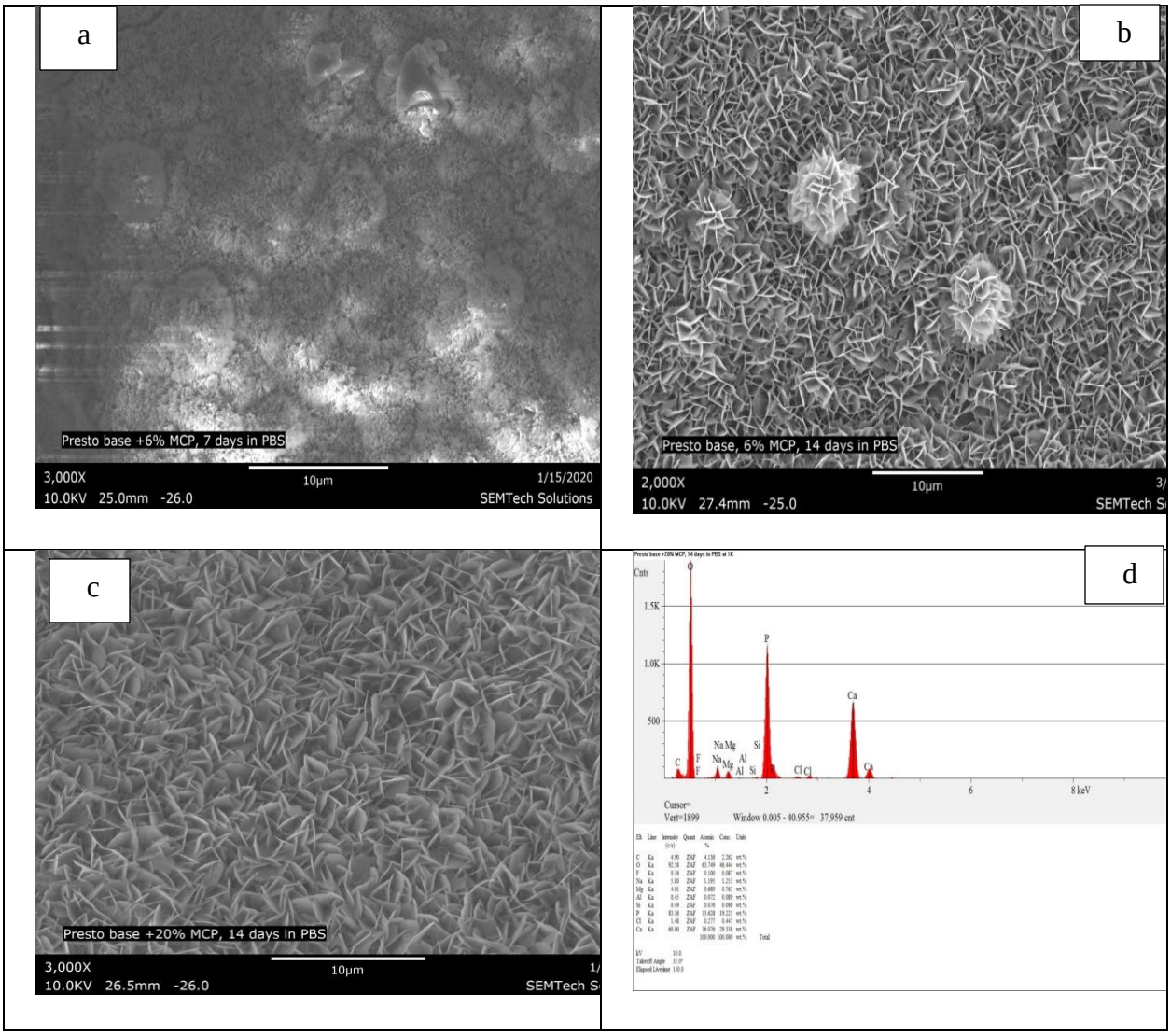

Figure 7. (a) SEM micrograph of specimen containing 6 Wt.% MCP (**CS-6**) after emersion in PBS for 7 days shows amorphous phases (the reduced quality of the micrograph may be attributed to the short range order of the amorphous CaP and the accidental inclusion of water (3,000x); (b) SEM of specimen with **CS-6** after 14 days of immersion in PBS shows the well-developed CaP crystals (2,000x); (c) SEM of specimens containing 20% MCP (**CS-20**) after immersion in PBS for 14 days shows fully developed CaP crystals (3,000x); (d) EDS data of specimen with **CS-20** after 14 days storage in PBS shows CaP ratio of 1.6, which is the stoichiometric ratio for hydroxyapatite.

Preprints (www.preprints.org) | NOT PEER-REVIEWED | Posted: 16 May 2021 doi:10.20944/preprints202105.0363.v1

DISCUSSION

The crystallinity and solubility of calcium phosphate can be controlled by adding suitable additives to the reactants [39]. It is known that the addition of organic or polymeric materials serves to stabilize calcium and phosphate, as these prevent agglomeration and control crystallite growth [22]. Compared to crystalline calcium phosphates, amorphous calcium phosphate exhibits greater bioactivity and has been shown to have better adhesion to periodontal ligament cells [40]. The incorporation of the organic monomer, Bis-2, as a functional reactant to synthesize MCP creates better solubility and stability for the calcium phosphate. MCP has greater solubility compared to the commercial grade HAp or the commercial grade dicalcium phosphate [41]. Furthermore, MCP has moderate solubility in hydrophilic monomers that enables it to generate a homogeneous phase that can act as a translucent, esthetic, mono-block composite.

The optical and physical properties of dental composites are highly influenced by the composition of the resin matrix and fillers. Variables include (i) the resin matrix type and its amount, (ii) the size, shape and amount of inorganic fillers, (iii) the interaction of the resin matrix and the fillers, and (iv) the amount and type of the photo-initiator system. [42, 43] Translucency and opacity have been viewed as vital properties of esthetic dental composite resins. They are the indicators of the quality and quantity of the reflected light, and they have a profound effect on the cure efficiency [44], i.e., the degree of conversion and the depth of cure. It is reasonable to assume that a highly translucent, resin-based composite has a higher degree of conversion, transmits light deeper into the material, and has a greater depth of cure [45] than a less translucent material.

The degree of conversion is an important tool to determine the final physical, mechanical, and biological properties of dental composites. The correlation between the degree of conversion and the mechanical performance of photopolymerized dental composites has been well studied

 doi:10.20944/preprints202105.0363.v1

[43]. The degree of conversion of the dental composite resin determines the success of direct restorations: (i) greater monomer to polymer conversion corresponds to superior mechanical properties, and (2) greater conversion may result in less uncured, potentially leachable monomers in the composite [46].

Depth of cure of dental composites is clinically relevant and is defined as "the thickness of a resin that may be converted from a monomer to a polymer, under a specific light curing condition" [47]. Depth of cure serves as a reference for placing the material in increments without compromising the physical and biological properties of the material. Similar to translucency and degree of conversion, depth of cure is highly influenced by the resin matrix, the photo-initiator system, and the nature of the filler.

In this study, all composite formulations contained the same resin composition, photo-initiator system, inorganic fillers, and shade to investigate the effect of the added MCP filler on translucency, degree of conversion, and depth of cure. It was found that replacing some of the inorganic filler with an equal amount of MCP improved the translucency parameter, increased the depth of cure, and showed a similar degree of conversion over that of a control composite without MCP. The higher translucency parameter and depth of cure of a composite with 3 Wt.% MCP is attributed to the higher interaction and solubility of the MCP filler with the resin phase. Composite with 6 Wt.% MCP exhibited a lower mean degree of conversion of 64% and slightly lower depth of cure, but had similar mean translucency parameter as the control composite with no MCP. On the other hand, composite with 20 Wt.% MCP showed the lowest mean value for translucency parameter (5.5), degree of conversion (58%), and a mean depth of cure (2.48 mm). All tested composites have acceptable depths of cure for clinical application.

 doi:10.20944/preprints202105.0363.v1

The mean flexural strength of the composites with MCP filler wase tested by a three-point ISO 4049 method. Composite with 3Wt.% MCP presented the highest flexural strength (106 MPa), which was slightly higher than that of the control composite (98.2MPa). The composite with 6Wt% MCP showed slightly higher mean flexural strength compared to the control composite, but the difference is not statistically different. The composite with 20Wt% MCP showed the lowest mean flexural strength of 92.6 MPa. The lower values are attributed to the lower degree of conversion due to the high paste viscosity and reduced filler-resin interaction. All composite formulations exhibited good toughness values, which are evidenced by high flexural strength and high deflection at break. The high toughness of the dental composites studied in the present work is attributed to the incorporation of the rubberized urethane in the resin matrix of the composite formulation. Composites with higher toughness and flexural properties enhance the fatigue strength and longevity of dental restorations [26, 48]. The high flexural strength and toughness of the 3 Wt.% MCP specimens is further confirmed by their low wear and high polishability [41].

The ion releasing properties of the experimental composites with MCP were studied in distilled water over a period of four weeks. The ion release data is presented as micrograms of ions released per cm^2. Dental composites that release adequate amounts of calcium and phosphate ions have been demonstrated to achieve dentin lesion remineralization [49]. A recent study demonstrated that the high phosphate content in BioGlass increases apatite formation and promotes osteogenesis [50]. In an earlier study, the authors reported that a 3 Wt.% MCP composite releases and recharges fluoride, calcium and phosphate ions [41]. In the present study, the effect of varying amounts of MCP on the release of calcium and phosphate ions was investigated. The release of phosphate and calcium ions from the dental composites was directly correlated to the amount MCP in the composites.

Preprints (www.preprints.org) | NOT PEER-REVIEWED | Posted: 16 May 2021 doi:10.20944/preprints202105.0363.v1

The present study also shows a direct correlation between the amount of crystalline calcium phosphate precipitated on the surface of the specimen and the length of time the specimen was stored in the PBS.

The biomineralization pathway of MCP containing composites is different from that of Bioglass 45S5 or that of calcium-silicate based dental products. In Bioglass 45S5 and calcium-silicate based products, such as TheraCal (Bisco, Schaumburg, IL USA) and MTA (Septodont, Cedex, France), there is a rapid release of soluble ionic species (Ca^{+} and Si^{+} ions) from the glass; a polycondensation reaction of surface silanols to generate a large number of heterogeneous nucleation sites; and crystallization of biologically reactive hydroxyl carbonate apatites in contact with a phosphate-containing medium (saliva) [51]. In MCP containing composites, the presence of ionic resins (Bis-2) plays a crucial role in the biomineralization of calcium phosphate and mediates the stabilization of the inorganic calcium phosphate nano-crystals. Based on the observation of higher bioactivity in MCP containing composites, even at lower weight percentage in the material, one could suggest the biomineralization pathway of the MCP containing composites proceeds through a matrix-particle-mediated process assisted by the acidic phosphate monomer present in the composite.

The role of the experimental composites polyionic resin matrix on the biomineralization process can be further understood by application of various theories proposed by researchers [8, 52, 53]. Also to be considered are: (1) the role of phosphoproteins on the biomimetic templating and stabilization of calcium phosphates [54]; (2) the role of non-collagenous protein (NCP) analogues, such as phosphonic acid and polyacrylic acid, in bio-mineralization [55]; and (3) the role of bio-composites of calcium deficient hydroxyapatite and amino acids [56]. The authors speculate that the ionic phosphate groups in the experimental composite resin matrices highly

Preprints (www.preprints.org) | NOT PEER-REVIEWED | Posted: 16 May 2021 doi:10.20944/preprints202105.0363.v1

influence the growth of calcium phosphate crystals and the bioacivity of the composites. The enhanced bioactivity of the experimental composites is further explained by the addition of seed particles of MCP, which upon reaction with the phosphate resin, form calcium deficient hydroxyapatite nucleation sites for the growth of biological calcium phosphate crystals [57].

It was noted that highly crystalline calcium phosphate was formed on the surface of composites containing 6 Wt.% MCP after 14 days of immersion in PBS. This is evidenced in the FTIR spectrum by the characteristic absorption peaks of crystalline calcium phosphate at 1094 cm^{-1}, 1029 cm^{-1}, 963 cm^{-1}, 603 cm^{-1}, and 563 cm^{-1}**.** It is also evidenced in the EDS data **(Table 4)**, which indicates the bio-mineralization of CaP is going through an amorphous calcium phase, with a Ca:P ratio less than 1.40, on the way to a highly crystalline HAp, with a Ca:P ratio of 1.6, as reported by various researchers.

Calcium phosphate fillers without polymerizable vinyl or methacrylate functional groups lack chemical interaction with the resin phase; their interactions are solely mechanical in nature. The presence of the pendant, polymerizable, methacrylate group in MCP has the advantage of covalently attaching the MCP fillers to polymer resin composites by taking part in free-radical polymerization with vinyl- or methacrylate-functional co-monomers. This chemically modified reinforcement of calcium phosphate creates a more intimate contact with the resin phase, resulting in a dental material that can readily transfer its loads between its resin and filler phases. The superior mechanical properties of the experimental composites with MCP are attributed to the better chemical integration of MCP with the resin phase.

 doi:10.20944/preprints202105.0363.v1

CONCLUSION

The present work details the synthesis of Methacrylate-functionalized Calcium Phosphate (MCP) and its efficient use as a bioactive filler in dental and biomaterial composites. The incorporation of MCP as a bioactive filler in esthetic dental composite formulations and its ability to promote precipitation of hydroxyapatite on the surfaces of those composites was evaluated. The progress of the nucleation and crystal growth of calcium phosphate on the surface of the composites was investigated by SEM/EDS with respect to the percentage of MCP in the composite and with respect to the immersion time in PBS. It was found that there is a direct correlation between the amount of MCP in a composite formulation and the deposition of hydroxyapatite on the material's surface.

The bioactivity of MCP, and its role in an ionic resin to create a nucleation template, was investigated. Methacrylate-functionalized calcium phosphate (MCP) enables the creation of highly-mineralized, durable, polymer-based composites with mono-functional, di-functional or multi-functional monomers. Dental restorative materials with MCP as a bioactive filler may provide better protection against micro-leakage and secondary caries without sacrificing esthetics and mechanical properties.

REERENCES

[1] Halgas, R.; Dusza,J.; Kaiferova, J.; Kovacsova, L.; Markovska, N. Nanoindentation testing of human enamel and dentin. *Ceramics Silikaty* **2013**, 57(2), 92-99.

[2] Linde, A.; Goldberg, M. Dentinogenesis. *Crit. Rev. Oral Bio Med.* **1993,** 4(5), 679-728.

[3] George, A.; Veis, A. Phosphorylated proteins and control over apatite nucleation, crystal growth, and inhibition. *Chem. Rev.* **2008**, 108 (11), 4670–4693. .https://doi.org/10.1021/cr0782729

[4] Abou Neel, E.; Aljabo, A.; Strange, A.; Ibrahim, S.; Coathub, M.; Young, A.; Bozec, L.; Mudera, V. Demineralization-remineralization dynamics in teeth and bone, *Int. J. Nanomed.* **2016**, 11, 4743-4763.https://doi.org/10.2147/IJN.S107624

[5] White, D.J. The application of in vitro models to research on demineralization and remineralization of teeth. *Adv. Dent. Res.* **1995**, 9(3), 175-193. https://doi.org/10.1177/08959374950090030101

[6] Featherstone, J.D.B. The continuum of dental caries- Evidence for a dynamic disease process. *J. Dent. Res.* **2004**, 83, C39-42.

[7] Langhorst, S.E.; O'Donnell, J.N.R.; Skrtic, D. In vitro remineralization of enamel by polymeric amorphous calcium phosphate composite: Quantitative micro radiographic study. *Dent. Mater.* **2009**, 25(7), 884–891. https://doi.org/10.1016/j.dental.2009.01.094

[8] Liang, K.; Wang, S.; Tao, S.; Xiao, S.; Zhou, H.; Wang, P.; Cheng, L.; Zhou, X; Weir, M.D,; Oates, T.W.; Li, J.; Xu, H.H.K. Dental remineralization via Poly (amido amine) and restorative materials containing calcium phosphate nanoparticles. *Int. J. Oral Sci.* **2019**, 11(15), 1-12. https://doi.org/10.1038/s41368-019-0048-z

[9] Chen, L.; Shen, H.; Suh, B.I.; Bioactive Dental Restorative Materials: A Review. *Am. J. Dent*. **2013**, 26(4), 219-27.

[10] Dorozhkin, S.V. Calcium orthophosphates in dentistry. *J Mat Sc.: Mater. Med.* **2013**, 24, 1335-1363. https://doi.org/10.1007/s10856-013-4898-1

[11] Abedi-Amin, A.; Luzi, A.; Giovarruscio, M.; Paolone, G.; Darvizeh. A.; Agullo, V.V.; Sauro, S. Innovative root-end filling materials based on calcium-silicates and calcium-phosphates. *J. Mat. Sci: Mater. Med.* **2017**, 28, 31. https://doi.org/10.1007/s10856-017-5847-1

:

[12] Okazaki, M.; Ohmae, H. Mechanical and biological properties of bioactive resin apatite composite resins. *Biomater*ials **1988**, 9(4), 345-348.

[13] Skrtic, D.; Antonucci, J. M.; Eanes, E. D. Amorphous Calcium Phosphate-Based Bioactive Polymeric Composites for Mineralized Tissue Regeneration. *J. Res. Natl. Inst. of Stand. Technol*. **2003**, *108*(3), 167–182. https://doi.org/10.6028/jres.108.017

[14] J.N.R. O'Donnell, J.N.R.; Schumacher, G.E.; Antonucci,J.M.; Skrtic, D. Structure-Composition-Property Relationships in Polymeric Amorphous Calcium Phosphate-Based Dental Composites. *Materials* **2009**, 2(4), 1929-1954 https://doi.org/10.3390/ma2041929.

[15] Mehdawi, I.; Neel, E.A.A.; Valappil, S.P.; Palmer, G.; Salih, V.; Pratten, J.; Spratt, D.A.; Young, A.M. Development of remineralizing antibacterial dental materials. *Acta. Biomater*. **2009**, 5 (9), 2525-2529. https://doi.org/10.1016/j.actbio.2009.03.030.

[16] Aljabo, A.; Neel, E.A.A.; Knowles, J.C.; Young, A.M. Development of dental composites with reactive fillers that promote precipitation of antibacterial-hydroxyapatite layers. *Mater. Sci. Eng. C*: **2016**; 60 (1): 285-292.https://doi.org/10.1016/j.msec.2015.11.047

[17] Wang, Y.; Zhu, M.; Zhu, X.X. Functional fillers for dental resin composites. *Acta. Biomater.* **2021**, 122 (1), 50-67.https://doi.org/10.1016/j.actbio.2020.12.001

[18] Santos, C.; Luklinska, Z.B.; Clarke, R.L.; Davy, K.W.M. Hydroxyapatite as a filler for dental composite materials: Mechanical properties and invitro bioactivity. *J. Mat. Sc.: Mater. Med.* **2001**, 12, 565–573. https://doi.org/10.1023/A:1011291723503

[19] Melo, M.A.S.; Guedes, S.F.F.; Xu, H.H.K.; Rodrigues, L.K.A. Nanotechnology based restorative materials for dental Caries management. *Trends Biotechnol*. **2013**, 31(8): 459-467. https://doi.org/10.1016/j.tibtech.2013.05.010

[20] Moreau, J.L.; Sun, L.; Chow, L.C.; Xu, H.H.K. Mechanical and acid neutralizing properties and bacteria inhibition of amorphous calcium phosphate dental nanocomposite. *J. Biomed. Mater. Res. B Appl. Biomate.r* **2011**, 98(1), 80-88. https://doi.org/10.1002/jbm.b.31834

[21] Natale, L.C.; Rodrigues, M.C.; Alania, Y.; Chiari, M.D.S.; Vilela, H.S.; Vieira, D.N.; Arana-Chavez, V.;Meier, M.M.; Vich,i F.M.; Braga, R.R. Development of calcium phosphate/ethylene glycol dimethacrylate particles for dental applications. *J. Biomed. Mater. Res. Part B* **2019**, 107 (3), 708-715. https://doi.org/10.1002/jbm.b.34164

[22] Rodrigues, M.C.; Chiari, M.D.S.; Alania, Y.; Natale, L.C.; Arana Chavez, V.E.; Meier, M.M.; Fadel, V.S.; Vichi, F.M.; Hewer, T.L.R.; Braga, R.R. Ion releasing dental restorative composites containing functionalized brushite nanoparticles for improved mechanical strength. *Dent. Mater.* **2018**, 34 (5) 746-755. https://doi.org/10.1016/j.dental.2018.01.026

[23] Chiari, M.D.S.; Rodrigues, M.C.; Pinto, M.F.C.; Vieira, D.N.; Vichi, F.M.; Vega, O.; Chrzanowski, W.; Nagoka, N.; Braga, R.R. Development of brushite particles synthesized in presence of acidic monomers for dental applications. *Mater. Sci. Eng. C*: **2020**,116, 111178. https://doi.org/10.1016/j.msec.2020.111178

[24] May, E.; Donly, K.J. Fluoride release and rerelease from a bioactive restorative material. *Am. J. Dent.* **2017**, 30(6), 305.

[25] Saunders, K.G.; Mattevi, G.; Donly, K.J.; Anthony, R. Enamel demineralization adjacent to orthodontic brackets bonded with ACTIVA BioACTIVE-RESTORATIVE. *APOS Trends Orthod.* **2018,** 8, 200-203.

[26] Pameijer, C.H.; Garcia-Godoy, F.; Morrow, B.R.; Jefferies, S.R. Flexural strength and flexural fatigue properties of resin-modified glass ionomers. *J. Clin. Dent.* **2015** 26(1), 23-25.

[27] ElReash, A.A.; Hamama, H.; Abdo ,W.; Wu, Q.; El-Din, A.Z.; Xioli, X. Biocompatibility of new bioactive resin composite versus calcium silicate cements: an animal study. *BMC Oral Health* **2019**, 19, 194. https://doi.org/10.1186/s12903-019-0887-1

[28] Maciak, M. Novel applications of a bioactive resin in perforations, root resorption and endodontic- periodontic lesions. *Roots* **2018**, 4, 32.

[29] Lopez-Garcia, S. et.al, In Vitro evaluation of the biological effects of Activa Kids bioactive restorative, Ionolux and Riva Light cure on Human dental pulpal stem cells. *Materials* **2019**, 12, 3694. https://doi.org/10.3390/ma12223694

[30] Skaria, S.; Berk, K. Stabilized calcium phosphate and methods of forming same **US patent 10,219,986** 03-05-2019.

[31] Skaria, S.; Berk, K. Radically curable urethane dimethacrylates and compositions thereof for tougher dental prosthetics **US patent 8, 292,625** 10-23-2012.

[32] Johnston, W.M. Review of translucency determinations and applications to dental materials, *J. Esthet. Restor. Dent.* **2014**, 26(4), 217-223. https://doi.org/10.1111/jerd.12112

[33] Wang X, Huyang G, Palagummi S, Liu X, Skrtic D, Beauchamp C, Bowen R, Sun J, High performance dental resin composites with hydrolytically stable monomers. *Dent. Mater.* **2018**; 34(2), 248-257.https://doi.org/10.1016/j.dental.2017.10.007

[34] ISO Standard 200: ISO 4049 Polymer based filling, restorative and luting materials. International Organization for Standards, 3rd edition.1-27.

[35] Raole, V.; Mashru, R.; Quantification of Anions and Cations in Restorative Biochemic tissue salts, *Public Health and Preventive Medicine* **2018**; 4: 129-147.

[36] **ISO 23317:2014 Implants for surgery. In vitro evaluation for apatite-forming ability of implant materials.2014-06.**

[37] Ramli, R.A.; Adnan, R.; Abu Bakar, M.; Masudi, S.M. Synthesis and characterization of pure nanoporous hydroxyapatite. *J Phys Sci*, **2011**, 22(1),25–37.

[38] Homaeigohar, S.; Tsai, T.Y.; Zaire, E.S.; Elbahri, M.; Young, T.H.; Boccaccini, A.R. Bovine Serum Albumin (BSA) / polyacrylonitrile (PAN) biohybrid nanofibers coated with a biomineralized calcium deficient hydroxyapatite (HA) shell for wound dressing. *Mater Sci Eng. C:* **2020**, 16, 111248. https://doi.org/10.1016/j.msec.2020.111248

[39] Antonucci, J.M.; Liu, D.W.; Skrtic, D. Amorphous calcium phosphate based composites: Effect of surfactants and poly(ethylene oxide) on filler and composite properties. *J. Dispers. Sci. Technol*. **2007**, 28(5), 819–824. https://doi.org/10.1080/01932690701346255

[40] Dorozhkin, S.V. Self setting calcium orthophosphate formulations and their biomedical applications. *Adv. Nano BioM&D* **2019**, 3(3), 321-421.

[41] White Pages: www.pulpdent.com. Properties of Presto™:

[42] Ferracane, J.L.; Greener, W.H. The effect of resin formulations on the degree of conversion and mechanical properties of dental restorative resins, .*J Biomed. Materl. Res.* **1986**, 20(1), 121-131. https://doi.org/10.1002/jbm.820200111

[43] Salgado, V.E.; Albuquerque, P.P.A.C.; Cavalcantec, L.M.; Pfeifer, C.S.; Moraes, R.R.; Schneider, L.P.J. Influence of photoinitiator system and nanofiller size on the optical properties and cure efficiency of model composites. *Dent. Mater.* **2014**, 30(10), e264-e271. https://doi.org/10.1016/j.dental.2014.05.019.

[44] Lee,Y.K. Translucency of human teeth and dental restorative materials and its clinical relevance. *J. Biomed. Opt.* **2015**, 20 (4), 0450016. .https://doi.org/10.1117/1.JBO.20.4.045002

[45] Salgado, V.E.; Rego, C.F.; Schneider, L.P.J.; Moraes, R.R.; Cavalcantec, L.M. Does translucency influence cure efficiency and color stability of resin-based composites. *Dent. Mater.* **2018**, 34(7), 956-967. https://doi.org/10.1016/j.dental.2018.03.019

[46] da Silva, E.M.; Poskus, L.T.; Guimaraes, J.G.A. Influence of Light-polymerization Modes on the Degree of Conversion and Mechanical Properties of Resin Composites: A Comparative Analysis Between a Hybrid and a Nanofilled Composite. *Oper. Dent.* **2008**, 33(9), 287-293. https://doi.org/10.2341/07-81

[47] Yap, A.U.J.; Pandya, M.; Toh, W.S. Depth of cure of contemporary bulk-fill resin-based composites. *Dent. Mater. J.* **2016**, 35(3), 503-510 https://doi:10.4012/dmj.2015-402

[48] Arola D, Fatigue testing of biomaterials and their interfaces. *Dent. Mater.* **2017**, 23 (11), 367-381. https://doi.org/10.1016/j.dental.2017.01.012

[49] Skrtic, D.; Antonnuci, J.M.; Eanes, E.D. Effect of the monomer and filler systems on the remineralizing potential of bioactive dental composites based on amorphous calcium phosphate. *Polym. Adv. Technol*. **2001**, 12(6), 369 -377. https://doi.org/10.1002/pat.119

[50] Li, Y.; Chen, L.; Chen, X.; Hill, R.; Zou, S.; Wang, M.; Liu,Y. High phosphate content in bioactive glasses promotes osteogenesis in vitro and in vivo. *Dent. Mater*. **2021**, 37(2), 272-283. https://doi.org/10.1016/j.dental.2020.11.017

[51] Hench, L.L.; Polak, J.M. Third-generation biomedical materials. *Science* **2002**, 295, 1014–1017. Hench, L. Bioactive Glass: Chronology, characterization, and genetic control of tissue generation in : B. Ben-Nissan [Ed] Advances in Calcium Phosphate Biomaterials, Springer Series in Biomaterials Science and Engineering -2, Springer, NY, (2014), 51-70.

[52] Cao, C.Y.; Mei, M.L.; Li, Q.; Lo, E.C.M.; Chu, C.H. Methods for biomimetic remineralization of human dentine: A systemic Review. *Int. J. Mol. Sci.* **2015**, *16*, 4615-4627. .https://doi.org/10.3390/ijms16034615

[53] He, L.; Hao, Y.; Li, Z.; Liu, H.; Shao,M.; Xu, X.; Liang, K.; Gao, Y.; Yuan, H.; Li, J. Li, J.; Cheng, L.; Loveren, C.V. Biomineralization of dentin. *J. Struct. Biol.* **2019**, 207, 115-122. https://doi.org/10.1016/j.jsb.2019.05.010

[54] Gluseren, G.; Tansik, G.; Garifullin, R. Dentin phosphoprotein mimetic peptide nanofibers promote biomineralization. *Macromol. Biosci*, **2019**, 19 (1),1800080. https://doi.org/10.1002/mabi.201800080

[55] Niu, L.; Zhang, W.; Pashley, D.H.; Breschi, L.; Mao, J.; Chen, J.; Tay, F.R. Biomimetic remineralization of dentin, *Dent Mater*. **2014**, 30(1), 1-35. .https://doi.org/10.1016/j.dental.2013.07.013

[56] Veis, A.; Dorvee, J.R. Biomineralization mechanisms: A new paradigm for crystal nucleation in organic matrices. *Calcif. Tissue Int*. **2013**, 93(4), 307–315. https://doi.org/10.1007/s00223-012-9678-2

[57] Jin, W.; Jiang, S.; Pan, H.; Tang, R. Amorphous phase mediated crystallization: Fundamentals of biomineralization. *Crystals*, **2018**, 8 (1), 48. https://doi.org/10.3390/cryst8010048